Heat Mass Transfer (2012) 48:1485–1493
DOI 10.1007/s00231-012-0992-z

ORIGINAL

Computational transport phenomena in bioprocessing with the approach of the optimized source term in the governing equations

Maria Valeria De Bonis · Gianpaolo Ruocco

Received: 7 June 2011 / Accepted: 5 March 2012 / Published online: 23 March 2012

Abstract Progress in the modeling of bio and food industry processes can be achieved by developing robust and efficient codes. Even complex configurations can be tackled, featuring multiphysics mechanisms that are interdependent or even competing with each other. In this paper the use of optimized "source terms" of the governing partial differential equations are discussed, reporting on simulation results. The related framework is addressed, as well as the potential of the adopted approach.

List of symbols

A_1 Pre-exponential term (1/s)
A_2 Exponential factor (m^3/mol)
c Molar concentration (mol/m^3)
D Diffusivity (m^2/s)
E_a Activation energy (J/mol)
K Reaction rate constant (1/s)
k_i Mass transfer coefficient (m/s)
k_w Wall reaction rate constant (m/s)
Q Thermal power (W)
R Universal gas constant (J/mol K)
S Generic source term
t Time (s)
T Temperature (K)
$\mathbf{v}$ Velocity vector (m/s)

Greek

α_1 Empirical constant (dimensionless)
δ_T Thickness of thermal layer (m)
ϕ Generic variable
ρ Density (kg/m^3)

M. V. De Bonis · G. Ruocco (✉)
CFDfood, DITEC Università degli Studi della Basilicata, Campus Macchia Romana, 85100 Potenza, Italy
e-mail: gianpaolo.ruocco@unibas.it

Subscript

0 Reference, nominal

1 Introduction

A variety of transport phenomena can be found in bio- and food engineering, and can be usefully studied to analyze and improve existing processes or pursue innovation. A vast body of fundamental and applied research is presently available, and many approaches have been proposed so far [31–34], but a simplification of these approaches may contribute to a broader comprehension of the intimate workings of food processes.

1.1 The mechanisms of mass, heat and momentum transport

Mass transfer can be defined as the migration of a substance through a substrate or mixture under a concentration gradient in order to reach chemical equilibrium [33, 34]. Mass transfer phenomena are found during thermal treatment of liquids, in frying, in convective or combined drying, and in the transfer of water vapor and gases in packaged substrates.

Heating on raw substrates is performed for various purposes, such as inhibition of the microbial population, inactivation of enzymes, reduction of the amount of water, that is, in cooking in general [31, 34]. Heating is often coupled to mass transfer, in all operations mentioned above. On the other hand heat is removed from foods by cooling and freezing, usually by forced convection, to reduce the rate of its deteriorative chemical and enzymatic reactions and again to inhibit microbial growth thereby

extending shelf life. In any case, knowledge is needed to achieve better control and avoid under- or over-processing, which often results in detrimental effects on functional and nutritional characteristics of substrates.

Finally, momentum transfer is also very frequent in the bio- and food industry as heat and/or mass transfer phenomena can occur in association with flow. When momentum transfer is analyzed in the fluid field some particular considerations should be taken into account [32, 34]. The type of food component, its concentration, its specific evalutive characteristics play important roles in the structure and engineering properties of each product.

1.2 Inherent difficulties in modeling and special formulations

Species concentration, temperature and velocity distributions are therefore ubiquitous in the processing at stake, but modeling difficulties arise as all transport mechanisms are usually intertwined and non-linearly interdependent, that is, they can be considered as coupled. An additional analytical effort is necessary to overcome the traditional limitation of imposing empirical notations as transfer coefficients, e.g. at the external surface of a substrate being exposed to a working fluid. To this end, a conjugate solution of the field variables could be computed regardless of the phases interface.

In some cases the substrate is far from being uniform in nature: porous and multi-phase modeling of bio-substrates has been exploited many times, starting from the seminal contributions due to Singh and his co-workers [13], and Ni and Datta [27]. An extensive body of literature on the subject of transport phenomena in porous media then followed [7, 19, 29], but the approaches are limited by the adoption of several empiricisms. Moreover, as noted by Mujumdar [24, 25], real food process modeling cannot be always generalized by the porous media assumptions, as bulk transport properties can already generally be referred to the macroscopical behavior of the substrate, and process are product-specific, involving chemical as well as physical transformations.

A different simplifying approach can be tried instead, describing the transport phenomena based on the classical partial differential equations (PDEs) ensemble for a homogeneous medium. This classical ensemble allows the sharing of many analytical similarities among the transport phenomena, therefore enjoying a relative ease of implementation when applied in this complex modeling framework.

1.3 Implementation in a generalized computational fluid dynamics workplace

Affordable solutions of a variety of models based on PDEs differential equations have been made possible by the development and availability of robust and efficient Computational Fluid Dynamics (CFD) codes to realize a flexible computing workplace. In particular, solutions of mechanical force, pressure, temperature, and/or velocity distributions, which act as driving forces of the transport phenomena of momentum and energy, as reviewed by Norton and Sun [28], can be addressed to infer their influence on bio-substrates, processes or even industrial plants. The same CFD workplace can complemented with adequate computational segments to specify for each biochemical occurrence at hand, such as inhibition of microbes, denaturation of vitamins, degradation of enzymes, as proposed by [1]. In this way, solutions of concentration distributions can be inferred as well, with all related dependencies on the other two transport phenomena, to realize a true "multiphysics" computing environment.

1.4 An optimized "kinetics-oriented" multiphysics solving system

In this paper the application of such an approach is presented, together with some typical case studies of bio and food processes. Multiple simultaneous physical phenomena are invoked by means of their governing PDEs (for velocity components, temperature, or chemical species ϕ) with the following general form [2]:

$$\frac{\partial \rho \phi}{\partial t} + \mathbf{v} \cdot \nabla \phi = D \nabla^2 \phi \pm S \tag{1}$$

where:

- the first term at the left-hand side is the temporal accumulation/depletion of ϕ in time, in the considered system;
- the second term at the left-hand side is the macroscopic/convective transport of ϕ;
- the first term at the right-hand side is microscopic diffusive transport of ϕ;
- the last term is the source term, on which special attention must be devoted for each specific framework, as presented in this paper.

Generally, when modeling the chemical species transport, the source term S can be described by the following Arrhenius expression:

$$S = K\phi \tag{2}$$

with

$$K = K_0 \exp^{-E_a/RT} \tag{3}$$

This generic kinetics notation can be usefully inserted in a governing PDE when proper kinetics assembly K_0 and E_a are addressed for each case. In the present paper, this approach has been employed to model a number of processes, with the advantage of a considerable modeling simplification.

With the present approach, the integration of the governing PDEs has been then complemented by using the design environment modeFRONTIER [23] in which a SIMPLEX [12] multi-object optimization routine is exploited to form the optimal kinetics assembly, or design constraints, in Eq. (3). Practically, n design constraints can be analyzed by calculating the following error function $f(x, e)$:

$$f(x,e) = (x_0 - e_0)^2 + (x_1 - e_1)^2 + (x_2 - e_2)^2 + \cdots + (x_n - e_n)^2 \tag{4}$$

with x_i the ith constraint variable and e_i the i th experimental validating datum. By this routine, a CFD kernel [6, 15] is iteratively run, until PDEs system convergence for a minimized error function f. Figure 1 illustrates a typical data flow of the employed CFD optimization.

2 Thermization of liquids by direct steam injection

Heat treatment is the major preservation mechanism that can be applied by the bio and food industry, to destroy microbial and enzyme activity and render products commercially sterile. Developments in processing technology aim to reduce the damage to nutrients and sensory components, such as with the direct steam injection (DSI). As recently reported by a US Patent by [26], DSI can be exploited to produce a sterile product and deliver liquid foods of high quality in a high temperature short time (HTST) process. DSI can be modeled by CFD, to show the directions for improved energy and functional efficiencies. However, no modeling is available in the available literature, except in [10] who reported on the interactions between fluid mechanics, heat transfer, and functional issues such as the evolution of bacteria and vitamins (or bio-indicators ϕ in Eq. (3)). With this approach, the attention can be precisely devoted to monitor the evolution of those bio-indicators.

A model has been therefore devised to describe transient, two-phase, multi-component diffusive and convective heat and mass transport in a axisymmetric control volume (Fig. 2), and was validated in [10] against the available data [26]. A concentrated citrus juice, j, comprised of liquid water and given bio-indicator concentrations, and a flow of

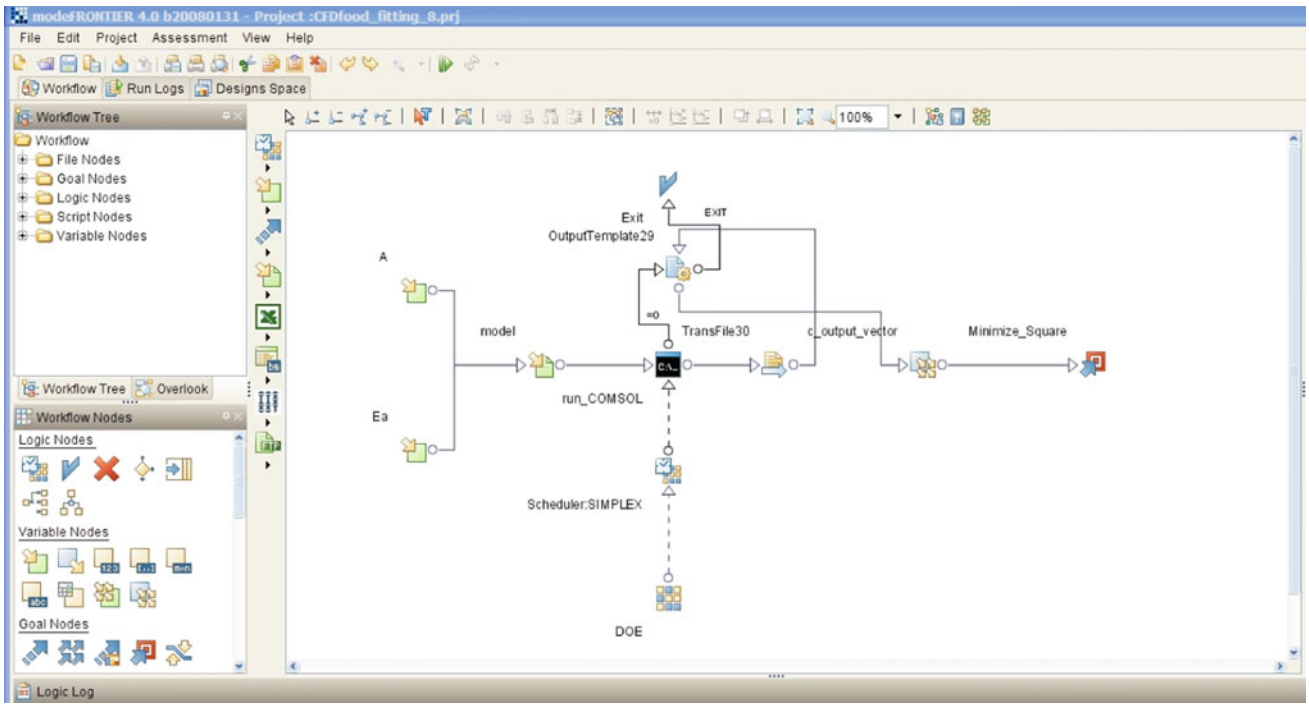

Fig. 1 A data flow by using modeFRONTIER [23] to optimize the kinetics assembly in a simulation of food drying. Based on a SIMPLEX routine, several A and E_a values form a Design of Experiment (DOE) base, which is iteratively tried and automatically entered in a COMSOL [6] kernel. The output vector validity is checked by minimizing a sum of squared differences, as explained by Eq. (4)

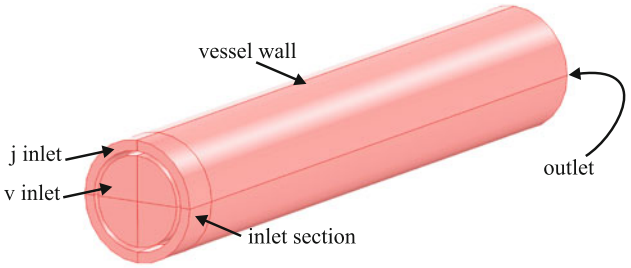

Fig. 2 DSI process simulation: the adopted vessel geometry [10]

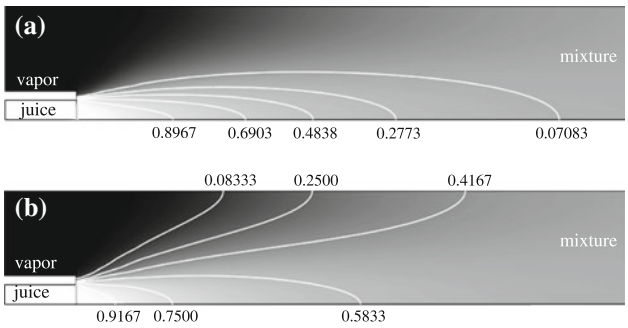

Fig. 3 DSI process simulation: qualitative temperature map in the axisymmetric geometry (*white* 353 K, *black* 394 K), with superimposed quantitative isocurves of **a** native bacteria and **b** original vitamin relative concentrations, in the initial part of the vessel [10]

dispersed saturated water vapor, v, are merged to realize a DSI configuration. Juice and vapor enter the reactor at their j and v inlet, respectively; downstream of the inlet sections, the juice is thermally treated by the vapor flow, then through the outlet the flow is sent to a successive cooling section.

The energy transport in the vessel determines the evolution of the two bio-indicators at hand: these can be therefore tracked down during and along the process.

The kinetics for bio-indicator evolution follows an Arrhenius, temperature-dependent form. In this case, the negative sign is applied to describe the inactivation of the bio-indicator, c_b (bacteria or vitamin):

$$S = -K_0 \exp\left(-\frac{E_a}{RT}\right) c_b \tag{5}$$

As reported in Fig. 3a, the bacteria are strongly inactivated in the upper part of the vessel, where the thermal action of the vapor is stronger. Due to a more responsive kinetics, this bio-indicator is therefore heavily affected by the treatment. In accord to [26], the time needed to reach the correspondent experimental 5-log reduction of *Alyciclobacillus acidoterrestris* count is only about 2 s.

In Fig. 3b the second bio-indicator distribution is reported: there, Vitamin C is denaturated where the temperature is higher, but due to a milder kinetics the macroscopic transport is more evident so that the original vitamin is carried over more easily downstream.

3 Heat exchanger fouling

Additionally to the control of the safety and quality, attention must be drawn upon the management of the treatment device as well. For example, during the thermal treatments of sensible fluid foods in common Plate Heat Exchangers (PHE), proteins are often degraded and precipitated to form fouling that greatly affect the treatment efficiency and alter the product's desired features [20]. CFD can then be exploited bringing forth temperature and velocity information, that yields for deposit distributions when coupled to biochemical notations for thermal denaturation of fluid constituents.

A pasteurization treatment of milk in the first channel passage of a PHE has been studied to analyze the βLactoGlobulin's (βLG) denaturation and subsequent aggregation, responsible for the PHE fouling. This model was validated in [9] by comparing the computations versus data from [17] for average fouling deposition. The transfer phenomena at hand are based on the βLG's local kinetics mechanisms and related time evolution, depending on the adopted thermal regime and flow geometry, and included in the CFD formalism. A specific reaction scheme of [20] is adopted to form D denaturated proteins from a N native one, and so on for A aggregated and F fouled protein deposit, by means of specific reaction rates K:

$$N \xrightarrow{K_{ND}} D \xrightarrow{K_{DA}} A \xrightarrow{K_{AF}} F \tag{6}$$

Species production/destruction fit into the standard driving mass transport equations, with the source term S of Eq. (2) dealing with the creation or destruction (positive or negative rate) reactions. Two PHE regions r are identified: the bulk fluid b or the thermal boundary layer l. As the adopted source term is based on the fluid arrangement, its form is more complicated than usual, depending also on each ij species coupling. For sake of completeness S is reported as follows:

$$S_{ij,r} = K_{ij,r} c_{i,r} - \frac{k_i}{\delta_T} \Delta^{bl} c_{i,r} \pm \frac{k_w}{\delta_T} c_{A,l} \tag{7}$$

Here $c_{i,r}$ are the species concentrations of the i species in the r region, $c_{A,l}$ is the species concentration of the aggregated protein in the l region, $\Delta^{bl} c_{i,r}$ is the difference between the values in the b and l regions for each species, $K_{ij,r}$ are the specific reaction rates in terms of Arrhenius expressions, and k_i and k_w are a mass transfer coefficient for each species and a wall reaction rate constant (an additive mass transfer coefficient) for the aggregated

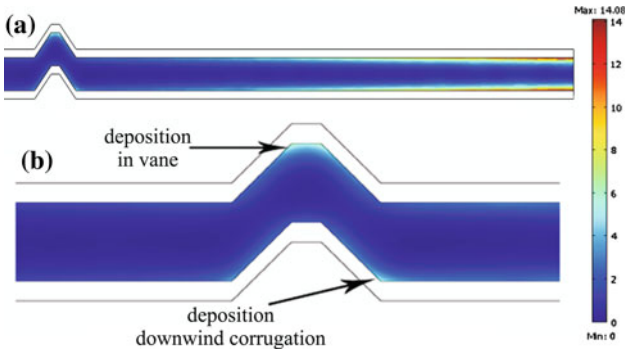

Fig. 4 Fouling simulation: fouling concentration (c_F) distribution at outlet (**a**) and a close-up near the last corrugation (**b**), with deposition loci 1 and 2 (in the 0–14 mol/m^3 range) [9]

protein in the boundary layer, respectively. The last term at the right-hand side is zero for all species except for the aggregated A and fouling F proteins.

Combining such kinetics in a CFD workplace, the standard unsteady-state governing Navier-Stokes and energy equations are applied to yield for variable in both fluid and deposit subdomains.

Fouling concentration c_F, velocity and temperature can be therefore described to test new corrugation shapes and orientations, to minimize the phenomenon. From this study βLG denaturation (i.e the thermal damage) is initiated in those regions where the fluid is slowed down and the contact time with heating walls is longer. As an example, in Fig. 4 the topology of the deposition is reported. Most of the fouling is created at channel outlet (Fig. 4a); some specific deposition loci appear also downwind of last corrugation and also in its corresponding vane (Fig. 4b), where small stagnation regions are found.

4 Formation of toxic chemicals

Frying is a complex heat treatment applied to many foods where several physical and chemical changes take place, such as size or shape, melting of fat, starch gelatinization, protein denaturation and water evaporation and transport. Heating also causes other important components such as free amino acids and sugars to react via the Maillard reaction and form chemical compounds, but some of these compounds may not be beneficial or may even be toxic to humans. In this circle, the formation of acrylamide (AA) occupies an important role; in fact, this molecule has been classified by the International Agency for Research on Cancer as probably carcinogenic to humans [3].

Food frying is eminently a conjugate process, meaning that the transfer of heat and chemical species must be modeled simultaneously in both solid and fluid phases and are strongly coupled through evaporation and properties variation on local temperature [18]. Such conjugate, biochemical evolution during cooking of some potato strips in olive oil can be worked out in which multiple, local transport phenomena mechanisms are applied to describe the thermal history and related biochemistry upon processing in [3] and [4]. This model is validated by comparing the computed data versus experimental measurements. In particular, the kinetics of AA formation is taken care of by imposing two source terms resulting from two consecutive reactions. Their schematic, from reactant sugars RS to AA-protein complex and to AA degradation product DP, is shown in the following, whereas K_{for} and K_{eli} are the first-order rate constants for molecule formation and elimination, respectively:

$$RS \xrightarrow{K_{for}} AA \xrightarrow{K_{eli}} DP \tag{8}$$

Equation (2) for S takes the form:

$$S = K_0 \exp\left[\frac{E_a}{R}\left(\frac{1}{T_0} - \frac{1}{T}\right)\right] c_{AA} \tag{9}$$

where T_0 and T are the reference and local substrate temperature, respectively and c_{AA} is the acrylamide molar concentration.

In Fig. 5 the AA local distribution is presented for two operating conditions: $T_p = 170$ °C with $\Delta t = 360$ s (Case I), and $T_p = 190$ °C with $\Delta t = 240$ s (Case II). In both explored cooking Cases AA has been forming and accumulating similarly, the greatest quantity to be found on the lateral side, confirming what determined for temperature in Fig. 6. The maximum c_{AA} is 5.0×10^{-3} or 2.9×10^{-2} mg/g for Case I or II at $\Delta t = 240$, respectively, while for the longer $\Delta t = 360$ s at $T_p = 170$ °C the maximum c_{AA} is 7.6×10^{-3} mg/g.

5 Combined microwave/thermal convection drying

Drying is one of the most common methods of preserving food, involving a complex combination of transport phenomena such as the application of heat and the removal of moisture, from a food substrate to a flow of auxiliary air. The decreased water content can be evaluated in relative terms as reduction of water activity to inhibit microbial growth and enzyme kinetics, and also to result in transport and storage costs reduction [14]. Understanding of local drying quality can help to improve process parameters and hence product quality, emphasizing on the external and internal process parameters that influence drying behavior [8].

In this context microwave (MW) treatments have been gaining increasing recognitions in the food industry and

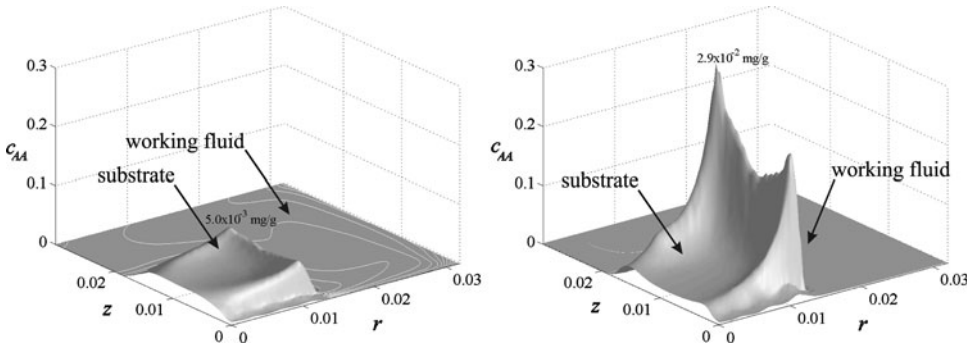

Fig. 5 Simulation of AA formation in deep frying of a potato sample: three-dimensional representation of c_{AA} (mg/g) in the entire domain, with indication of the maximum value, and superimposed isotherms, for $\Delta t = 360$ s and $T_p = 170$ °C (Case I, *left*) $\Delta t = 240$ s and $T_p = 190$ °C (Case II, *right*) [3]

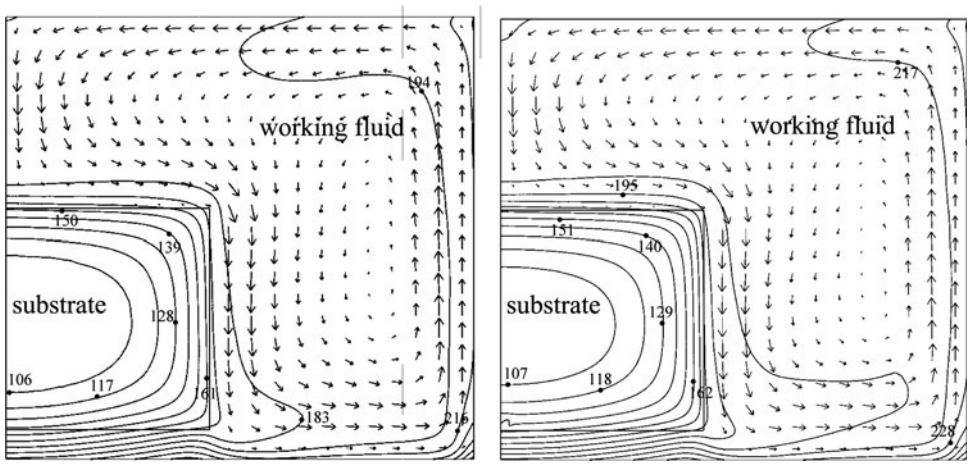

Fig. 6 Simulation of AA formation in deep frying of a potato sample: temperature T (°C) contour and velocity vector **u** (m/s) computed distributions for $T_p = 170$ (Case I, *left*) and 190 °C (Case II, *right*), after $\Delta t = 240$ s. Vector lengths are proportional to velocity intensity in the 0–0.0015 m/s range [3]

household frameworks alike. MW processing is recognized as a rapid treatment, nonetheless it is characterized by a certain non-uniformity in the temperature distribution. In fact, depending on the specific product's penetration depth, overheating loci can be attained near the sample's core, as reviewed in [22]. Therefore, better energy and finishing efficiencies can be obtained by adding an additional transport mechanism such as forced air convection heating [16].

A combined heating and drying by convection and MW can be studied by a conjugate model, exploiting a kinetics-based evaporation and a solution of the Maxwell's equation in a thin food substrate. This model has been validated in [22] with respect the available literature data [21]. The source term in the conductive heat transfer version of Eq. (1) has been written as a the sum of a generation term Q_{MW} and a evaporative cooling rate term Q_{EV}:

$$S = Q_{MW} - Q_{EV} \tag{10}$$

where Q_{MW} is the volumetric power due to dielectric dissipative effect of MW exposure given by:

$$Q_{MW} = Q_0 f(z) \tag{11}$$

Here Q_0 is the nominal incident MW volumetric power at the sample exposed surface, and the the dimensionless energy distribution $f(z)$ can be derived analytically from Maxwell's equations. The transfer of liquid water and water vapor in the substrate can be treated as well, with the same notations earlier implied to for the case of drying with a bulk air flow.

In Fig. 7 at left, the temperature T and moisture X distributions for the pure MW drying case ($T_p = 303$ K, $\mathbf{v}_p = 0$ m/s and $Q_0 = 250$ W with $t_p = 800$ s) are shown. The temperature distribution is practically uniform, and so it is also for the moisture, subject to a much faster evaporation rate, driven by the buoyant thermal plume. T and X are much affected by the natural convection, which is correctly modeled, for the environment stagnant air is still colder than the processed substrate.

The combined treatment ($T_p = 303$ K, $\mathbf{v}_p = 1.5$ m/s and $Q_0 = 250$ W with $t_p = 400$ s) depicted in Fig. 7, at right, holds the favorable features of both mechanisms instead: the substrate is treated faster that with the sole MW, but on the leading edge a moisture excess still exists. This is due to thermal mechanism dominance at the given

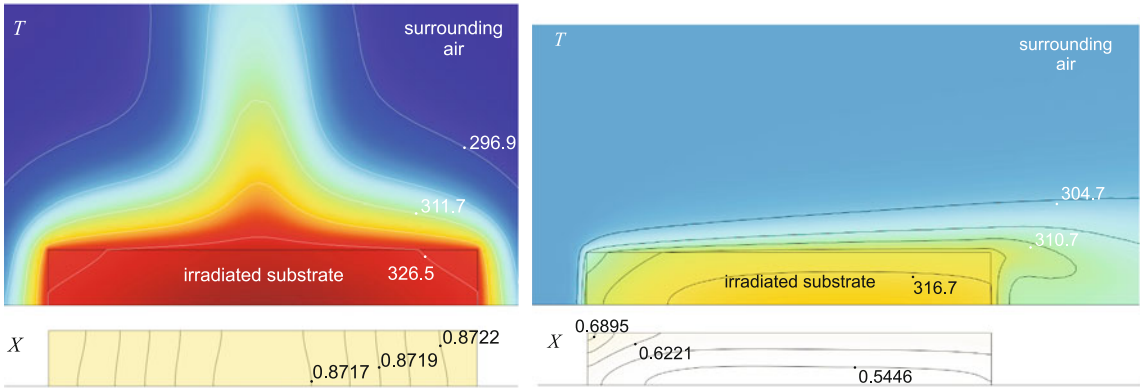

Fig. 7 Simulation of drying by a pure MW treatment (*left*), or by a combined treatment (*right*): T and X distributions after t_p = 400 s [22]

process duration: therefore the mechanism intensities (T_p and $\mathbf{v}_p$ for convection, and Q_0 for MW) must be adjusted for a more uniform treatment.

6 Modified atmosphere packaging

Specially arranged packaging gas, or Modified Atmosphere Packaging (MAP), coupled to low temperature storage, results in a prolonged shelf life of the fresh-cut fruit and vegetables. At the same time, quality is retained, safety is ensured and sales are promoted [35]. By using a MAP, produce respiration rate and related biochemistry are controlled: in particular, by raising CO_2 and/or reducing O_2 concentrations in packaging (protective atmosphere) or in refrigerated storage (controlled atmosphere).

Equations (1–3) are applied to a three-dimensional packaged space, containing 3 model, fresh-cut fruits, to describe each gas concentration, temperature and micro-organism count. The respiration of the product is taken care of by a simplified Michaelis–Menten relationship [11].

It can be seen that S includes the residual metabolism or additional deteriorative reactions promoted by the oxygen (such as pigment oxidation, senescence, enzymatic reactions and so on [30]), and depends on the local c_{CO_2}:

$$S = \alpha_l A_1 \exp(-A_2 c_{CO_2}) c_{O_2} \tag{12}$$

where α_l is an empirical constant which takes into account for the residual mechanisms, A_1 is a pre-exponential term and A_2 is the exponential factor accounting for the CO_2-induced respiration inhibition.

In this configuration, the headspace gas composition is altered solely by respiration as the packaging film has a selective species permeability to diffusion. With storage time, the evolution of concentrations is such that CO_2 increases at the expenses of O_2. The model is validated

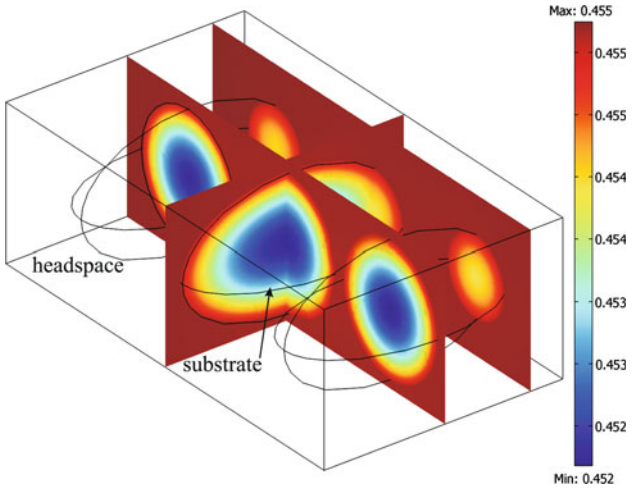

Fig. 8 Simulation of MAP: O_2 concentration map after 13 days of storage

with the experimental data reported in [5]. Figure 8 shows the O_2 distribution after 13 days of storage.

A microorganism kinetics of two bacteria populations (mesophilic, *MS*, and psychrophilic, *PS*) in a MAP modeling is included, based on their specific metabolism. Furthermore, most of the common spoilage bacteria and fungi require oxygen for growth therefore and its modeling is considered essential in the present context. The source therm for the bacteria must account for the dependence of the temperature and oxygen bio-availability, by means of a modified Arrhenius kinetics:

$$S_m = A_n \exp\left(\frac{-E_{a,n}}{RT}\right)\left(\frac{c_{O_2}}{c_{O_{2,i}}}\right) c_m \tag{13}$$

where c_m is the bacteria molar concentration.

Figure 9 shows that the microorganism distribution is not uniform: this is due to initial temperature gradient which affect the microbial growth. In fact, during the MAP

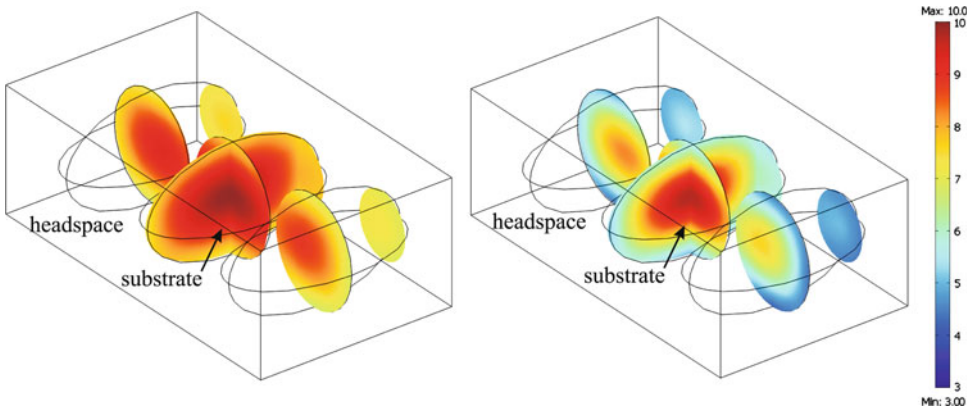

Fig. 9 Simulation of MAP: the MS (*left*) and PS (*right*) CFU maps after 13 days of storage

storage, the packaging ensemble is subject to cooling from post-harvest to the final temperature. Therefore the fruit core is the most contaminated zone, also confirmed by the oxygen depletion maximum which is seen at the fruit core.

7 Conclusions

The objective of this paper is to shed some light on the transport phenomena approach to modeling of many different food processes. The Computational Fluid Dynamics can be used as a tool to predict food processes as well as to design food processing equipment, specially when custom notations for biochemistry/multiphisycs are joined in the code, to support many industrial modeling needs.

Specific forms of the source term in the partial differential equations can account for the various frameworks at stake. Full coupled models can be applied for every different case, including realistic transfer exchange that are inherently allowing for food and working medium evolution. Bio-indicators can be tracked down in batch or continuous heat processing, to inform on the inherent quality, safety and operational configurations. Local drying quality can be monitored, even assisted by different physical mechanisms, to overcome the limitations of traditional approaches. Packaging or storage configurations can be studied by including the description of the subject produce metabolism.

References

1. AbdulGhani Al-Baali AG, Farid MM (2006) Sterilization of food in retort pouches. Springer, New York, NY
2. Bird RB, Stewart WE, Lightfoot EN (2002) Transport phenomena. Wiley, New York, NY
3. Carrieri G, De Bonis MV, Pacella C, Pucciarelli A, Ruocco G (2009) Modeling and validation of local acrylamide formation in a model food during frying. J Food Eng 95:90–98
4. Carrieri G, Anese M, Quarta B, De Bonis MV, Ruocco G (2010) Evaluation of acrylamide formation in potatoes during deep-frying: the effect of operation and configuration. J Food Eng 98:141–149
5. Cefola M, Renna M, Pace B (2011) Marketability of ready-to-eat cactus pear as affected by temperature and modified atmosphere. J Food Sci Technol.doi:10.1007/s13197-011-0470-5
6. COMSOL Multiphysics User's Guide (2009), COMSOL AB
7. Datta AK (2007) Porous media approaches to studying simultaneous heat and mass transfer in food processes. I: problem formulations. J Food Eng 80:80–95
8. De Bonis MV (2008) Analysis of food drying with the approach of interdependent transport phenomena. PhD Dissertation, Università degli Studi della Basilicata
9. De Bonis MV, Ruocco G (2009) Conjugate fluid flow and kinetics modeling for heat exchanger fouling simulation. Int J Therm Sci 48:2006–2012
10. De Bonis MV, Ruocco G (2010) Heat and mass transfer modeling during two-phase, continuous-flow processing of fluid food by steam heating. Int Commun Heat Mass 37:239–244
11. Del Nobile MA, Baiano A, Benedetto A, Massignan L (2006) Respiration rate of minimally processed lettuce as affected by packaging. J Food Eng 74:60–69
12. Edgar TF, Himmelblau DM, Lasdon LS (2001) Optimization of chemical processes, 2nd edn. McGraw-Hill, New York, NY
13. Farkas BE, Singh RP, Rumsey TR (1996) Modeling heat and mass transfer in immersion frying. I, model development. J Food Eng 29:211–226
14. Fellows PJ (2002) Food processing technology. CRC Press, Boca Raton, FL
15. FLUENT 6.3 User's Guide (2005), Fluent Inc
16. Geedipalli S, Datta AK, Rakesh V (2008) Heat transfer in a combination microwave–jet impingement oven. Food Bioprod Process 86:53–63
17. Georgiadis MC, Macchietto S (2000) Dynamic modelling and simulation of plate heat exchangers under milk fouling. Chem Eng Sci 55:1605–1619
18. Halder A, Dhall A, Datta AK (2007) An improved, easily implementable, porous media based model for deep-fat frying. Part I: model development and input parameters. Food Bioprod Process 85:209–219
19. Halder A, Dhall A, Datta AK (2007) An improved, easily implementable, porous media based model for deep-fat frying. Part II: results, validation and sensitivity analysis. Food Bioprod Process 85:220–230
20. Jun S, Puri VM (2006) A 2D dynamic model for fouling performance of plate heat exchangers. J Food Eng 75:364–374

21. Khraisheh MAM, McMinn WAM, Magee TRA (2000) A multiple regression approach to the combined microwave and air drying process. J Food Eng 43(4):243–250
22. Marra F, De Bonis MV, Ruocco G (2010) Combined microwaves and convestion heating: a conjugate approach. J Food Eng 97:31–39
23. ModeFRONTIER User's Guide (2008), ES.TEC.O. srl
24. Mujumdar AS (2006) Principles, classification, and selection of dryers. In: Mujumdar AS (eds) Handbook of industrial drying, 3rd edn, CRC press, Boca Raton, FL
25. Mujumdar AS (2007) An overview of innovation in industrial drying: current status and R&D needs. Transp Porous Med 66:3–18
26. Nasrallah M, Maldonado Perez A, Turndahl CJ (2008) Sterilization of flowable food products. US Patent 160149
27. Ni H, Datta AK (1999) Heat and moisture transfer in baking of potato slabs. Dry Technol 17(10):2069–2092
28. Norton T, Sun D-W (2007) An overview of CFD applications in the food industry. In: Sun D-W (eds) Computational fluid dynamics in food processing, CRC Press, Boca Raton, FL
29. Rahman SMA, Islam MR, Mujumdar AS (2007) A study of coupled heat and mass transfer in composite food products during convective drying. Dry Technol 25:1359–1368
30. Sandhya (2010) Modified atmosphere packaging of fresh produce: current status and future needs. LWT—Food Sci Technol 43:381–392
31. Sepúlveda DR, Barbosa-Cánovas GV (2002) Heat transfer in food products. In: Welti-Chanes J, Vélez-Ruiz JF, Barbosa-Cánovas GV (eds) Transport phenomena in food engineering, CRC Press, Boca Raton, FL
32. Vélez-Ruiz JF (2002) Introductory aspect of momentum transfer phenomena. In: Welti-Chanes J, Vélez-Ruiz JF, Barbosa-Cánovas GV (eds) Transport phenomena in food engineering, CRC Press, Boca Raton, FL
33. Welti-Chanes J, Mújica-Paz H, Valdez-Fragoso A, León-Cruz R (2002) Fundamentals of mass transport. In: Welti-Chanes J, Vélez-Ruiz JF, Barbosa-Cánovas GV (eds) Transport phenomena in food engineering, CRC Press, Boca Raton, FL
34. Welti-Chanes J, Vergara-Balderas F, Bermúdez-Aguirre D (2005) Transport phenomena in food engineering: basic concepts and advances. J Food Eng 67:113–128
35. Zhuang H (2011) Introduction. In: Brody AL, Zhuang H, Han JH (eds) Modified atmosphere packaging for fresh-cut fruits and vegetables, Blackwell, Oxford, pp 3–10